

The Characteristics and Function of Internalin G in *Listeria monocytogenes*

HUITIAN GOU^{1*}, YUANYUAN LIU¹, WENJING SHI¹, JINYU NAN², CHUAN WANG¹, YANAN SUN¹, QIHANG CAO¹, HUILIN WEI¹, CHEN SONG¹, CHANGQING TIAN¹, YANQUAN WEI¹ and HUIWEN XUE¹

¹ College of Veterinary Medicine, Gansu Agricultural University, Lanzhou, China

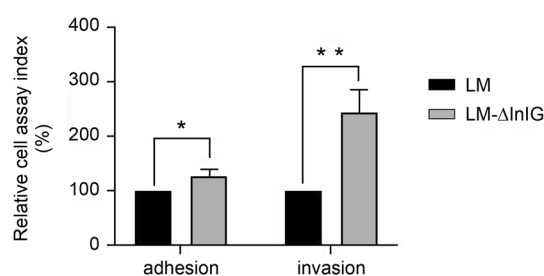
² Jiuquan City Animal Control Disease Center, Jiuquan, China

Submitted 22 November 2021, accepted 10 February 2022, published online 22 March 2022

Abstract

In order to clarify characteristics and function of internalin G (inlG) in *Listeria monocytogenes* ATCC[®]19111 (1/2a) (LM), the immune protection of the inlG was evaluated in mice, the homologous recombination was used to construct *inlG* deletion strains, and their biological characteristics were studied by the transcriptomics analysis. As a result, the immunization of mice with the purified protein achieved a protective effect against bacterial infection. The deletion strain LM-ΔinlG was successfully constructed with genetic stability. The mouse infection test showed that the virulence of LM was decreased after the deletion of the *inlG* gene. The deletion strain showed enhanced adhesion to and invasion of Caco-2 cells. Compared to the wild strain, 18 genes were up-regulated, and 24 genes were down-regulated in the LM-ΔinlG. This study has laid a foundation for further research on the function of *inlG* and the pathogenesis of LM.

In this study, immunization of mice with the purified inlG protein achieved a protective effect against *Listeria monocytogenes* infection. The virulence of LM-ΔinlG was decreased by mouse infection. However, the adhesion and invasion ability to Caco-2 cell were enhanced. Compared to the wild strain, 18 genes were up-regulated, and 24 genes were down-regulated in the LM-ΔinlG. This study has laid a foundation for further study of the function of the inlG and the listeriosis.



Keywords: *Listeria monocytogenes*, internalin G, immune protection, gene deletion, transcriptomics

Introduction

Listeria monocytogenes (LM) is an important zoonotic pathogen and one of the four food-borne pathogens, with a fatality rate of up to 30% (Wang et al. 2017; Radoshevich and Cossart 2018). Sixteen serotypes have been identified, and three are commonly involved in the infection, 4b and 1/2b in lineage I and 1/2a in lineage II (Datta and Burall 2018). As an intracellular bacterium, LM can stimulate the host's immune response and induce specific CD8⁺ and CD4⁺ T cell immune responses (Dowd et al. 2016). At present, LM poses a severe threat to human and animal health, primarily through frozen food, causing foremost food safety and public health concerns. Pregnant women, newborns, and the elderly are vulnerable to LM infec-

tion. Humans are mainly infected with LM through the fecal-oral route, and through eyes, mucous membranes, and damaged skin (Matle et al. 2020). The process of LM invasion into host cells is complex and involves multiple protein molecules such as pathogenic factors, adhesion molecules, and internalins (Pizarro-Cerdá and Cossart 2018).

Internalins are a protein family of LM. At present, there are 25 members, among which inlA and inlB are the earliest identified proteins related to bacterial invasion and are the main factors involved in bacterial invasion of host cells (Ireton et al. 2021). InlA mediates the internalization of LM through its interaction with the host-specific receptor E-cad, enabling LM to be endocytosed and enter the host epithelial cells (Drolia and Bhunia 2019). InlB can interact with multiple receptors

* Corresponding author: H. Gou, College of Veterinary Medicine, Gansu Agricultural University, Lanzhou, China; e-mail: gouht@gsau.edu.cn
©2022 Huitian Gou et al.

This work is licensed under the Creative Commons Attribution-NonCommercial-NoDerivatives 4.0 License (<https://creativecommons.org/licenses/by-nc-nd/4.0/>).

on the surface of host cells to mediate LM adhesion and invasion of hepatocytes and nonphagocytes (Al-Obaidi and Desa 2018). Only some internalins play a role in mediating LM invasion (Gouin et al. 2019; Mir 2021). Balandyté et al. (2011) found that the *inlG* protein was mainly present in environmental isolates and rarely in strains isolated clinically from human and animal samples, suggesting that *inlG* is closely related to LM survival in the external environment. Jia et al. (2007) found that the *inlG* accounted for 41.1% of the 236 isolates of LM. Jiang et al. studied 133 isolates of LM and found that *inlG* did not exist in lineage I but was present in 74.2% of lineage II, and 30.7% of lineage III (Jianjun 2011). However, there have been few studies on the role of *inlG* in LM invasion of host cells.

In the present study, *inlG* was expressed in a prokaryotic system. After immunizing mice with the expressed product, its protection was evaluated. An *inlG* deletion strain was constructed, and the phenotype of the deletion strain was studied through growth characteristics, hemolysis test, cell adhesion, cell invasion, and mouse infection to achieve a preliminary understanding of the biological function of *inlG*.

Experimental

Materials and Methods

Cell and plasmid. The reference strain of LM ATCC[®]19111 (1/2a) and human colorectal adenocarcinoma (Caco-2) cells were purchased from the China Culture Collection Center. *Escherichia coli* competent cells BL21 (DE3), prokaryotic expression plasmid pET-28a (+), and LM shuttle plasmid pKSV7 were preserved in our laboratory. The primers used for cloning *inlG* and the construction of the deletion strain LM-AinlG are shown in Table I.

Prokaryotic expression of *inlG*. To grow LM ATCC[®]19111 strains, overnight cultures were diluted 100-fold in Brain Heart Infusion medium (BHI, China)

and shaken at 37°C. The recombinant plasmid pET-28a (+)-*InlG* was constructed, which was transformed into the expression strain BL21 (DE3). We carried out IPTG induction to positive recombinant plasmid pET-28a (+)-*InlG* and optimization of the expression conditions, SDS-PAGE analysis of the expression product size, and western blotting to verify the antigenicity of the expressed protein.

Immunoprotection test of *inlG* in mice. Thirty-two 7-week-old male BALB/c mice were obtained from the Experimental Animal Center of the Chinese Academy Agricultural of Sciences (Lanzhou, China) and maintained in cages with food and water ad libitum. They were divided into two groups of 16 mice, respectively. Groups were immunized with 100 µg of recombinant *inlG* mixed with complete Freund's adjuvant (Sigma, USA) for priming and incomplete Freund's adjuvant (Sigma, USA) for boosting. Immunizations were carried out on days 1, 15, and 30. Blood was collected by tail vein bleeding before immunization. The antibody titer was measured after each immunization by indirect ELISA. When the titer increased more than 1:52,000, mice were intraperitoneally infected with LM at twice LD₅₀, and the immunoprotective effect of *inlG* on mice was evaluated by measuring the survival rate of mice.

Histopathological observation of mice. Mice in the three groups (unchallenged, unimmunized-challenged, and immunized-challenged) (n = 3, respectively) were dissected after death, and brain and liver tissues were removed and prepared in paraffin sections. After hematoxylin-eosin staining, pathological changes were observed under an optical microscope (Olympus, Japan).

Construction of the *inlG* deletion strain. The primers were designed to amplify the upstream and downstream homologous arms of the *inlG* gene. The homologous arm of AinlG was amplified with gene splicing by overlap extension PCR (SOE-PCR). After sequencing, the homologous arm of AinlG was linked to the shuttle plasmid pKSV7 to form the recombinant plasmid pKSV7-AinlG. The pKSV7-AinlG was transferred into

Table I
PCR primers used in the experiments.

Primer	Sequence	Product (bp)
ΔInlG-F1	CGGGATCCGCTTATGATACAGTAGAAGAA (<i>Bam</i> HI)	633
ΔInlG-R1	CCTCCGATGAAAAGCGTTCCTAAAATAGTAGGAATAATCCCAAGATAGCTGTCCT	
ΔInlG-F2	ATGTTTACTTGTAGTGACAGCTATCTTGGAATTATTCCTACTATTTTAGGAACGC	596
ΔInlG-R2	GCTCTAGAAGATAATTCAAGTTCTGTTA (<i>Xba</i> I)	
D-F	TGTCCGCAACAGCTAGCCCAG	1,644/3,100
D-R	GCAAGTGGGGTTAAATCACTT	
Hly-F	GATGCATCTGCATTCAATAA	1,510
Hly-R	TTATTCGATTGGATTATCTAC	

LM competent cells by Gene Pulser MXcell™ (BioRad, USA), and the positive bacteria were screened. Homologous recombination was carried out at 41°C in the presence of chloramphenicol. After complete recombination, the pKSV7 plasmid was lost under 30°C and no-chloramphenicol conditions. The genetic stability of the gene deletion strain was tested by PCR.

Phenotypic identification of LM-*inlG*. The growth of wild-type LM and LM-*inlG* was evaluated by measuring OD₆₀₀ at 30°C, 37°C, and 41°C and pH 5, 7, and 9. The adhesion and invasion rates of the two strains were calculated as described previously (Medeiros et al. 2021; Pereira et al. 2021). Human colon carcinoma cells (Caco-2) were cultured in Dulbecco's modified Eagle's medium (DMEM) (Gibco, China) with high glucose, supplemented with 10% fetal bovine serum (FBS) (Gibco, China). They were then seeded in 12-well plates at a density of 1×10^5 cells/well and incubated at 37°C in the presence of 5% CO₂. For the adhesion assay, overnight (18 h)-grown bacterial cultures were washed thrice with PBS, adjusted to OD₆₀₀ = 0.12, and suspended in DMEM to a final concentration of 1×10^8 CFU/ml. The Caco-2 cell monolayer was washed three times using DMEM, then exposed separately to the LM and LM-*inlG* and incubated for 2 h at 37°C under the atmosphere with 5% CO₂. After incubation, cells were washed three times with PBS and lysed using 500 µl of cold 0.5% Triton X-100. For the invasion assay, the monolayers were exposed to LM and LM-*inlG*, washed as performed in the adhesion assay, and treated with gentamicin (100 µg/ml, 1 h) and with 0.5% Triton X-100 (37°C, 10 min). The lysed cell suspensions from both adhesion and invasion experiments were serially diluted in PBS, and the bacterial concentration in the samples was determined by the number of colony-forming units (CFU). The adhesion/invasion efficiency (%) for each strain was calculated as the number of bacteria attached/invaded to the cells compared with the total number of CFU provided in the inoculation samples multiplied by 100. However, the LD₅₀ of mice for the deletion strain was determined the same as the wild strain.

Transcriptomics analysis of LM and LM-*AinlG*. Total RNA was extracted from LM and LM-*AinlG* samples using the RNeasy Pure Kit (Qiagen, China), following the manufacturer's instructions. In total, 5 µg RNA/sample was sent to Beijing Novogene Technology Co., Ltd., China for RNA sequencing. According to the instructions, the Library Prep Kit (Qiagen, China) was used to construct the chain-specific library for RNA samples. The library was sequenced using the Illumina sequencing platform (HiSeq 4000). Raw data (raw reads) of FASTQ format were firstly processed through in-house Perl scripts. The LM reference genome (NC_003210) and associated gene annotation

information were downloaded from the NCBI database. The sequence alignment software, Bowtie2 (2.3.4.3) was used for genome location analysis of clean reads.

The number of gene counts per sample was standardized using DESeq2 (1.20) software. We then performed hypothesis testing and set the threshold as $|\log_2 \text{Fold Change}| > 1$, p_{adj} value (corrected p -value) < 0.05 to screen out DEGs between LM and LM-*AinlG*. To systematically analyze gene biological function and genome information, the clusterProfiler (3.8.1) software was used for Gene Ontology (GO) function enrichment and the Kyoto Encyclopedia of Genes and Genomes (KEGG) pathway analysis for DEGs. p -Values were calculated and selected p_{adj} values were set to < 0.05 to determine the significant gene enrichment (Liao et al. 2019).

Results

Prokaryotic expression of *inlG*. The molecular weight of the *inlG* protein was estimated to be 53 ku, but the size of the *inlG* protein was about 70 ku according to SDS-PAGE. Therefore, the expressed protein was identified by mass spectrometry. The mass spectrometry results matched the LM reference sequence to the highest degree, and the protein was confirmed to be an expression product of the *inlG* gene. LM-positive serum was used as the primary antibody, and sheep anti-rabbit IgG was used as the secondary antibody. Western blotting showed that the induced protein had potential reactivity (Fig. 1).

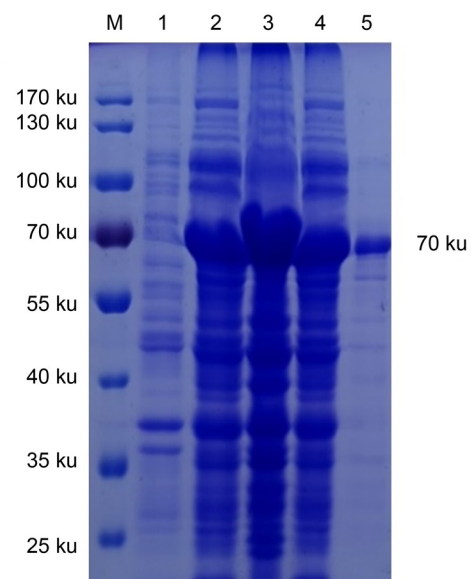


Fig. 1. Analysis of the recombinant protein. M – Protein marker, 1 – bacteria before the induction with IPTG, 2 – the induced bacteria, 3 – supernatant of lysed induced bacteria, 4 – precipitation of induced bacteria, 5 – purified *InlG* recombinant protein, 6 – uninduced bacteria reaction with positive serum, 7 – induced bacteria reaction with positive serum.

Table II
Determination of the median lethal dose of the bacteria (BACT) in mice.

BACT (CFU)	Death/Total	Mortality (%)
10^9	9/10	90
10^8	8/10	80
10^7	6/10	60
10^6	4/10	40
10^5	2/10	20
0	0/10	0

Immunoprotection test of inlG in mice. The mortality of mice infected with LM is shown in Table II and was calculated according to the formula: $\log LD_{50} = [Xm - i (XP - 0.5)]$. Finally, the LD_{50} of LM was $1.0 \times 10^{6.6}$ CFU. The antibody titer of inlG was more than 1:52,000 in mice by indirect ELISA. After intraperitoneal infection of mice with LM, the control group had rough hair and were huddled and listless. Individual mice gradually developed tremors, increased secretion at the canthus, and accelerated respiratory rate. Fifteen mice died within 72 h, and one survived. However, eight mice in the test group developed similar symptoms and died. The remaining eight mice became normal at 48 h after the challenge (Table II).

Histopathological observation of mice. Compared with the brain tissue of the normal group (Fig. 2a), the

challenge group after immunization with saline was filled with red blood cells, and a large number of lymphocytes were infiltrated in the pons (Fig. 2b). After protein immunization, the interface between the cortex and medulla in the brain tissue of mice in the challenge group was clear, and there were fissure vacuoles in the medulla (Fig. 2c). Brain tissue damage in the immunoprotein group post-challenge was milder than that in the normal saline group.

Compared with liver tissue in the normal group (Fig. 2d), mice in the challenge group after immunization with saline (Fig. 2e) suffered a severe liver injury, irregular arrangement of hepatic lobules, and dilated central veins. The hepatic cord of mice in the challenge group disappeared after protein immunization (Fig. 2f). As in the brain, liver injury in the protein challenge group was milder than in the normal saline challenge group.

Construction of LM-AinlG. The amplified upstream and downstream homologous arms of *inlG* were 633 and 596 bp, respectively. The homologous arms of the *inlG* were fused by SOE-PCR, and a fragment of 1,229 bp was obtained, which was named AinlG. The pKSV7 plasmid was ligated with AinlG by *Bam*HI and *Xba*I double digestion, and the product was transformed into DH5a competent cells. The recombinant plasmid pKSV7-AinlG was transformed into LM competent cells by electric shock and cultured at 30°C

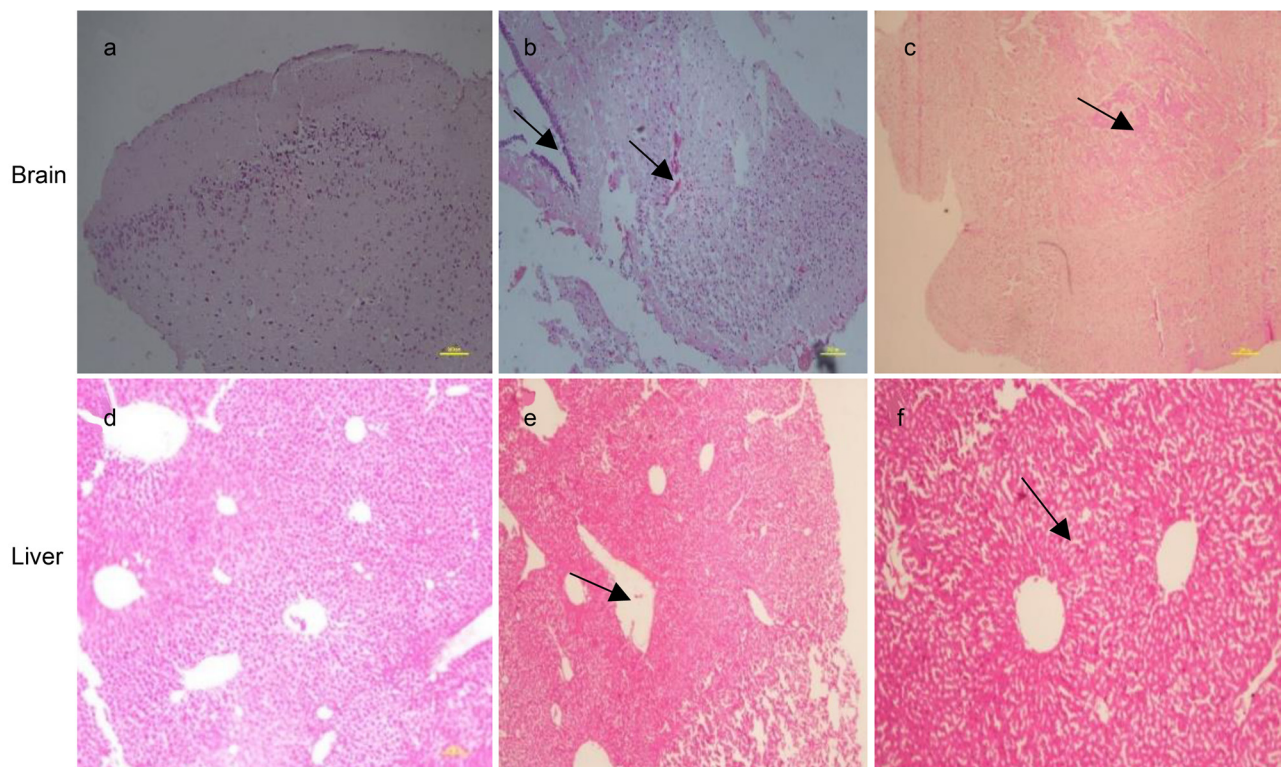


Fig. 2. Pathological changes in the tissue of infected mice stained with hematoxylin-eosin. a/d – Normal mouse, b/e – the mice immunized with normal saline, c/f – the mice immunized with protein and challenged with bacteria.

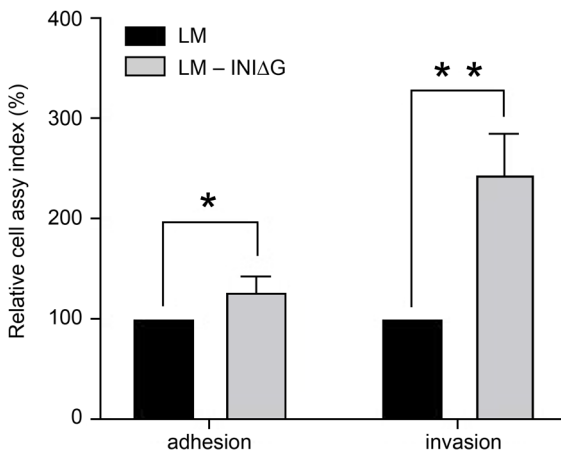


Fig. 3. Relative adhesion and invasion of LM and LM-ΔInlG in Caco-2 cells. This test was done in triplicate in each run and repeated for three times. The cell assay rates of LM19111 were set at 100%. * $p < 0.05$; ** $p < 0.01$.

with chloramphenicol. The positive transformants were screened and amplified as 1,229 bp. At the 70 th generation, the homologous recombination was completed.

The shuttle plasmid was lost successfully at the 30 th generation under the condition of 30°C and no antibiotics. The recombinant strain was cultured at 37°C for 20 generations, and a genetically stable deletion strain was finally obtained.

Biological characteristics of LM-AinlG. There was no significant difference in growth characteristics and biochemical and hemolysis test results between wild-type LM and LM-AinlG. The LD_{50} of the deleted strain LM was $1.0 \times 10^{6.9}$ CFU, and the wild strain LM was $1.0 \times 10^{6.6}$ CFU. The adhesion rate of LM-AinlG to Caco-2 cells was 1.3 times higher than the wild-type strain, and the invasion rate was about 2.45 times higher than the wild-type strain (Fig. 3).

Transcriptomic results of LM and LM-AinlG. The transcribed genes were classified into gene ontology (GO) categories: 45 genes were classified into biological processes, 19 to cellular components, and 29 to molecular functions. Compared to the wild strain, 18 genes were up-regulated and 24 genes were down-regulated in the LM-AinlG (Fig. 4). The DEGs were compared

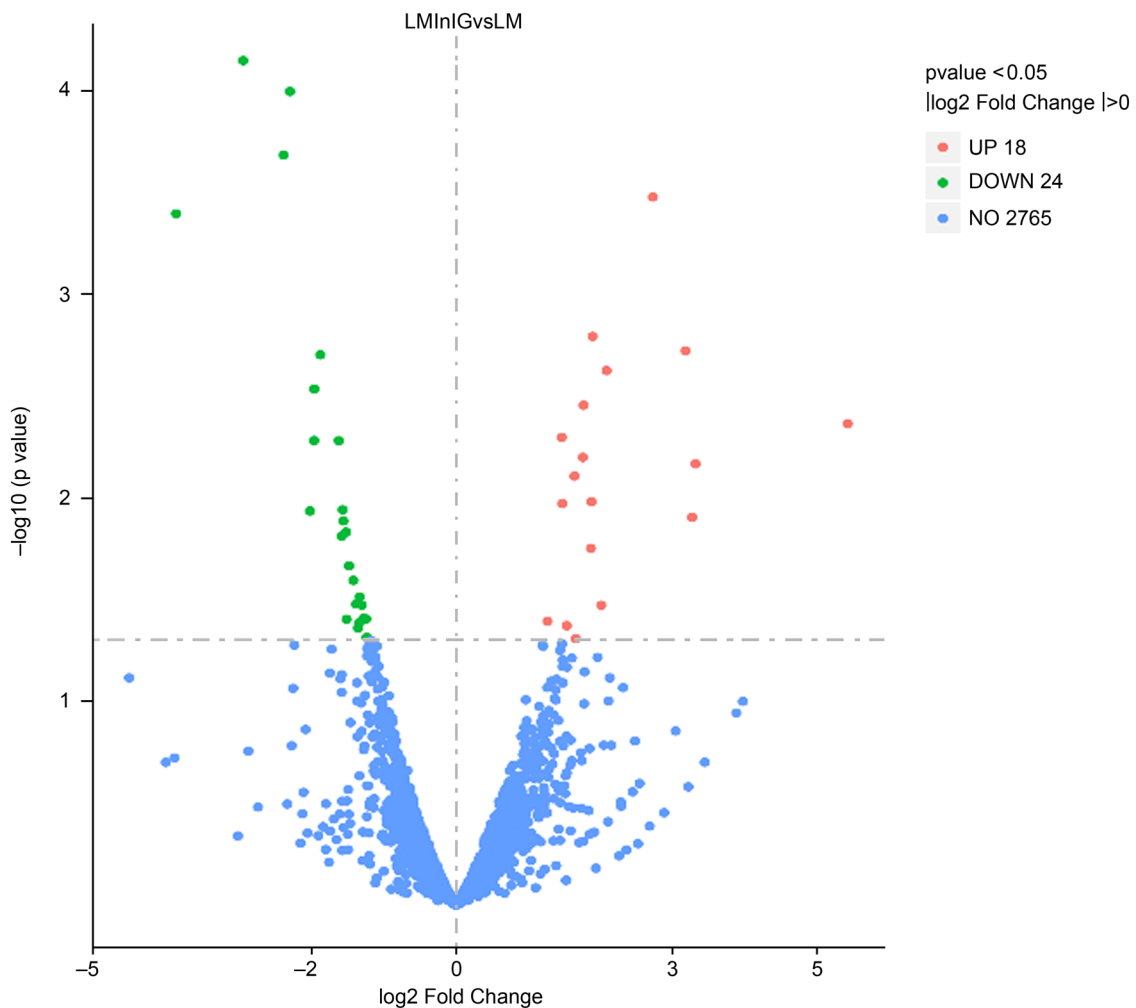


Fig. 4. Differentially expressed genes in LM-ΔInlG compared to LM. The abscissa indicates the fold change of gene expression, and the ordinate indicates the significance of the gene difference. The red dots indicate the up-regulated genes, the green dots indicate the down-regulated genes, and the blue dots indicate the genes that are not significantly different.

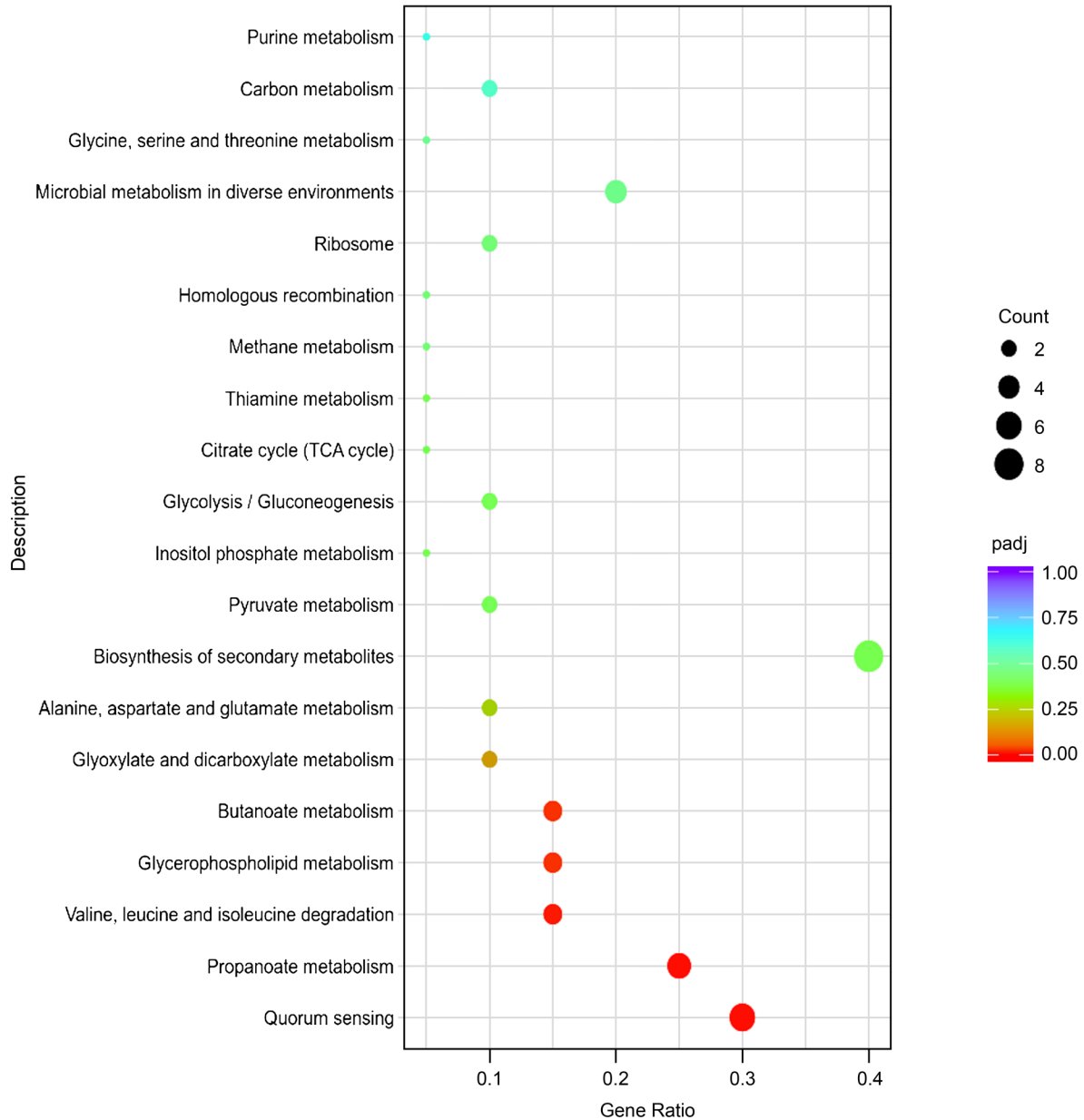


Fig. 5. KEGG pathway analysis of differentially expressed genes in LM- Δ InlG compared to LM. The enriched KEGG categories are on the vertical axis. The ratio of the enriched DEGs in the KEGG category to the total genes in that category is shown on the horizontal axis.

with the Kyoto Encyclopedia of Genes and Genomes (KEGG, <http://www.genome.jp/kegg>) and GO databases (<http://www.geneontology.org>). In Fig. 5, the abscissa represents the enrichment factor; the vertical coordinate represents the enriched function of the KEGG term. The larger the circle, the more differential genes are enriched to this function. Twenty metabolic pathways were enriched in the LM- Δ InlG (Fig. 5). Quorum sensing, Propanoate metabolism, Valine, leucine, and isoleucine degradation, Glycerophospholipid metabolism, Butanoate metabolism are the five significant KEGG enriched pathways from LM- Δ InlG compared LM (Table III).

Discussion

The *inlG* gene product consists of 490 amino acids, and the predicted molecular weight was about 53 ku. However, SDS-PAGE found the *inlG* protein to be about 70 ku, with a difference of 17 ku from the predicted molecular weight. After identifying *inlG* protein by mass spectrometry, the highest matching score was the LM reference sequence. The reason for this deviation between the experimental results and the predicted molecular weight may be the influence of the molecular weight standards of proteins at different concentrations of SDS-PAGE. After boiling, the denatured protein

Table III
Differentially expressed genes in related KEGG pathways in LM-ΔInlG compared to LM.

Term	Gene ID	Name	Log ₂ FC	Type	Description
Quorum sensing	lmo0205	plcB	1.89	up	phospholipase C
	lmo0202	hly	1.77	up	listeriolysin O precursor
	Novel00001	no	1.76	up	thiol-activated cytolysin
	Novel00002	no	1.64	up	thiol-activated cytolysin beta sandwich domain
	lmo2363	no	-1.35	down	glutamate decarboxylase
	lmo0447	no	1.66	up	pyridoxal-dependent decarboxylase conserved domain
Propanoate metabolism	lmo1373	no	-1.86	down	transketolase, pyrimidine binding domain
	lmo1153	no	1.88	up	propanediol dehydratase subunit alpha
	lmo2720	no	-2.02	down	AMP-binding enzyme C-terminal domain
	lmo1374	no	-1.52	down	biotin-requiring enzyme
	lmo1371	no	-1.28	down	pyridine nucleotide-disulphide oxidoreductase
Valine, leucine, and isoleucine degradation	lmo1373	no	-1.86	down	transketolase, pyrimidine binding domain
	lmo1374	no	-1.52	down	biotin-requiring enzyme
	lmo1371	no	-1.28	down	pyridine nucleotide-disulphide oxidoreductase
Glycerophospholipid metabolism	lmo0205	plcB	1.89	up	phospholipase C
	lmo1176	eutC	3.18	up	ethanolamine ammonia-lyase small subunit
	lmo1175	eutB	1.87	up	ethanolamine ammonia-lyase large subunit
Butanoate metabolism	lmo1369	no	-2.94	down	phosphate acetyl/butyryl transferase
	lmo2363	no	-1.35	down	glutamate decarboxylase
	lmo0447	no	1.66	up	pyridoxal-dependent decarboxylase conserved domain

forms a rod-like structure, and the surface uniformly adsorbs ions. Due to amino acid composition and other reasons, different proteins do not conform to this basic assumption (Matsumoto et al. 2019).

In the mouse protective test, the mortality was 93.75% in the control group and 50% in the experimental group, indicating that InlG protein conferred some antigenic protection after immunization. The cause of death of mice in the experimental group was analyzed. The LM used in this study was the highly pathogenic 1/2a serotype. Studies have reported that >98% of listeriosis is caused by serotype 1/2b, 4b, and 1/2a strains, and serotype 1/2a is the dominant strain in China (Chen et al. 2020; Liu et al. 2020). In addition, it may be related to the weak protection of mice immunized with InlG protein. Bu et al. (2017) found that the protection of recombinant fusion antigen was better than that of a single protein in mice challenged with LM. Therefore, the genes with dominant epitopes in the internalin family can be expressed in the future to study whether they have good antigenicity.

The internalins are closely related to LM virulence and are unique to LM for adhesion and invasion of host cells. In this study, *inlG* deletion had little effect on the growth characteristics and environmental tolerance of LM. The LD₅₀ of LM-ΔInlG was $1.0 \times 10^{6.9}$ CFU and that of LM was $1.0 \times 10^{6.6}$ CFU, indicating that the toxicity of LM-ΔInlG was decreased. However, after the deletion

of *inlG*, the adhesion to and invasion of Caco-2 cells were enhanced, which was consistent with that after the deletion of *inlC* (Jianjun 2011). During LM intracellular infection cycle, listeriolysin O (LLO, encoded by the *hly* gene) mediates LM escape from phagosomes through lysed phagocytic vacuole and membrane perforation (Lecuit 2020). PlcB can help LM escape from host autophagy clearance by inhibiting the maturation of autophagy precursors or preventing target recognition by autophagy mechanisms (Mitchell et al. 2018). ActA recruits actin nucleated complexes in the cytoplasm to induce actin aggregation to form pseudopod-like structures termed 'listeriopods', enabling LM to escape from autophagy of the host, driving the movement of LM in the cytoplasm and between cells, and entering neighboring host cells for a new round of adhesion and invasion (de las Heras et al. 2011). InlC, as a member of the internalins family, relaxes junctional tension through interaction with a regulator of the tight junction complex (TUBA), and aids LM to invade neighboring cells (Costa et al. 2020).

From the transcriptomics result of LM-ΔInlG compared to LM, the expression level of LLO, PlcB, ActA, and InlC were up-regulated. So, this result explains why the adhesion to and invasion of Caco-2 cells were enhanced for LM-ΔInlG. KEGG annotation results indicated that quorum sensing, propanoate metabolism, valine, leucine, and isoleucine degradation, glycerophospholipid

metabolism, and butanoate metabolism are significant pathways from LM-AinlG compared to LM. The quorum sensing (QS) pathway refers to the ability of bacteria to secrete signal molecules to the outside world continuously. By detecting the concentration of signal molecules, we can sense the population density of bacteria. QS regulates many biological characteristics, such as motility, biofilm formation, colonization, adhesion, virulence factor secretion, and bioluminescence, which are necessary for the survival or virulence of many bacteria (Younis et al. 2016). Amino acid metabolism, such as valine, leucine, and isoleucine metabolism, is likely critical for protein synthesis. However, the study also demonstrated that valine, leucine, and isoleucine degradation might be related to cell adhesion (Chandrashekar et al. 2020). Enrichment of propanoate metabolism may affect energy metabolism. These KEGG pathways were also observed in other bacteria and human cells, suggesting that propanoate may control the activity or stability of enzymes involved in pathways and affect energy metabolism regulation (Yi and Xie 2021).

Conclusions

This study evaluated the potential of *inlG* as a vaccine candidate to protect against LM infection. In addition, by constructing the gene deleted strain, it was verified that *inlG* was related to the virulence of LM. We also clarified the mechanism of LM-AinlG from the transcriptomics analysis. The next step will be to explore the detailed functional mechanism of *inlG* by analyzing the receptor for *inlG* and whether it acts synergistically with other internalins.

Availability of data and material

All raw sequences and analyzed data for this study have been deposited in the NCBI's GEO database as the accession number PRJNA783511.

Ethical statement

All experiments were approved by the college of Veterinary Medical, Gansu Agricultural University, China.

Acknowledgments

This work was supported by Gansu Agricultural University Youth Tutor Support Fund (GAU- QDFC-2020-10), the National Nature Science Foundation of China (No. 31960726, No. 32060822, and No. 31560700), Key Research and Development Program of Gansu Province (No. 20YF8FA136), National Key Research and Development Program of China (No. 2019YFC1605705). We are indebted to international science editing for the critical correction of this manuscript.

Conflict of interest

The authors do not report any financial or personal connections with other persons or organizations, which might negatively affect the contents of this publication and/or claim authorship rights to this publication.

Literature

- Al-Obaidi MMJ, Desa MNM.** Mechanisms of blood brain barrier disruption by different types of bacteria, and bacterial-host interactions facilitate the bacterial pathogen invading the brain. *Cell Mol Neurobiol.* 2018 Oct;38(7):1349–1368. <https://doi.org/10.1007/s10571-018-0609-2>
- Balandyté L, Brodard I, Frey J, Oevermann A, Abril C.** Ruminant rhombencephalitis-associated *Listeria monocytogenes* alleles linked to a multilocus variable-number tandem-repeat analysis complex. *Appl Environ Microbiol.* 2011;77(23):8325–8335. <https://doi.org/10.1128/AEM.06507-11>
- Bu RE, Wang JL, Wu JH, Xilin GW, Chen JL, Wang H.** Indirect enzyme-linked immunosorbent assay method based on *Streptococcus agalactiae* rSip-Pgk-FbsA fusion protein for detection of bovine mastitis. *Pol J Vet Sci.* 2017 Mar 1;20(2):355–362. <https://doi.org/10.1515/pjvs-2017-0043>
- Chandrashekar DS, Golonka RM, Yeoh BS, Gonzalez DJ, Heikenwälder M, Gerwirth AT, Varambally S, Vijay-Kumar M.** Fermentable fiber-induced hepatocellular carcinoma in mice recapitulates gene signatures found in human liver cancer. *PLoS One.* 2020 Jun 19;15(6):e0234726. <https://doi.org/10.1371/journal.pone.0234726>
- Chen S, Meng F, Sun X, Yao H, Wang Y, Pan Z, Yin Y, Jiao X.** Epidemiology of human listeriosis in China during 2008–2017. *Foodborne Pathog Dis.* 2020 Feb 01;17(2):119–125. <https://doi.org/10.1089/fpd.2019.2683>
- Costa AC, Pinheiro J, Reis SA, Cabanes D, Sousa S.** *Listeria monocytogenes* interferes with host cell mitosis through its virulence factors InlC and ActA. *Toxins (Basel).* 2020 Jun 20;12(6):411–415. <https://doi.org/10.3390/toxins12060411>
- Datta AR, Burall LS.** Serotype to genotype: the changing landscape of listeriosis outbreak investigations. *Food Microbiol.* 2018 Oct;75:18–27. <https://doi.org/10.1016/j.fm.2017.06.013>
- de las Heras A, Cain RJ, Bielecka MK, Vázquez-Boland JA.** Regulation of *Listeria* virulence: PrfA master and commander. *Curr Opin Microbiol.* 2011 Apr;14(2):118–127. <https://doi.org/10.1016/j.mib.2011.01.005>
- Dowd GC, Bahey-el-din M, Casey PG, Joyce SA, Hill C, Gahan CGM.** *Listeria monocytogenes* mutants defective in gallbladder replication represent safety-enhanced vaccine delivery platforms. *Hum Vaccin Immunother.* 2016 Aug 02;12(8):2059–2063. <https://doi.org/10.1080/21645515.2016.1154248>
- Drolia R, Bhunia AK.** Crossing the intestinal barrier via *Listeria* adhesion protein and internalin A. *Trends Microbiol.* 2019 May; 27(5):408–425. <https://doi.org/10.1016/j.tim.2018.12.007>
- Gouin E, Balestrino D, Rasid O, Nahori MA, Villiers V, Impens F, Volant S, Vogl T, Jacob Y, Dussurget O, et al.** Ubiquitination of *Listeria* virulence factor InlC contributes to the host response to infection. *MBio.* 2019 Dec 24;10(6):e02778–e19. <https://doi.org/10.1128/mBio.02778-19>
- Ireton K, Mortuza R, Gyanwali GC, Gianfelice A, Hussain M.** Role of internalin proteins in the pathogenesis of *Listeria monocytogenes*. *Mol Microbiol.* 2021 Dec;116(6):1407–1419. <https://doi.org/10.1111/mmi.14836>
- Jia Y, Nightingale KK, Boor KJ, Ho A, Wiedmann M, McGann P.** Distribution of internalin gene profiles of *Listeria monocytogenes* isolates from different sources associated with phylogenetic lineages. *Foodborne Pathog Dis.* 2007 Jun;4(2):222–232. <https://doi.org/10.1089/fpd.2006.0081>
- Jianjun J.** Disruption of InlC2 enhances the internalization of *Listeria monocytogenes* by epithelial cells. [PhD Thesis]. Shihezi (China): Shihezi University; 2011.
- Lecuit M.** *Listeria monocytogenes*, a model in infection biology. *Cell Microbiol.* 2020 Apr;22(4):e13186. <https://doi.org/10.1111/cmi.13186>

- Liao Y, Wang J, Jaehnig EJ, Shi Z, Zhang B.** WebGestalt 2019: gene set analysis toolkit with revamped UIs and APIs. *Nucleic Acids Res.* 2019 Jul 02;47 W1:W199–W205. <https://doi.org/10.1093/nar/gkz401>
- Liu Y, Sun W, Sun T, Gorris LGM, Wang X, Liu B, Dong Q.** The prevalence of *Listeria monocytogenes* in meat products in China: A systematic literature review and novel meta-analysis approach. *Int J Food Microbiol.* 2020 Jan;312:108358. <https://doi.org/10.1016/j.ijfoodmicro.2019.108358>
- Matle I, Mbatha KR, Madoroba E.** A review of *Listeria monocytogenes* from meat and meat products: Epidemiology, virulence factors, antimicrobial resistance and diagnosis. *Onderstepoort J Vet Res.* 2020 Oct 09;87(1):e1–e20. <https://doi.org/10.4102/ojvr.v87i1.1869>
- Matsumoto H, Haniu H, Komori N.** Determination of protein molecular weights on SDS-PAGE. *Methods Mol Biol.* 2019; 1855: 101–105. https://doi.org/10.1007/978-1-4939-8793-1_10
- Medeiros M, Castro VHL, Mota ALAA, Pereira MG, De Martinis ECP, Perecmanis S, Santana AP.** Assessment of internalin A gene sequences and cell adhesion and invasion capacity of *Listeria monocytogenes* strains isolated from foods of animal and related origins. *Foodborne Pathog Dis.* 2021 Apr 01;18(4):243–252. <https://doi.org/10.1089/fpd.2020.2855>
- Mir SA.** Structure and function of the important internalins of *Listeria monocytogenes*. *Curr Protein Pept Sci.* 2021 Dec 22;22(8): 620–628. <https://doi.org/10.2174/1389203722666210902163300>
- Mitchell G, Cheng MI, Chen C, Nguyen BN, Whiteley AT, Kianian S, Cox JS, Green DR, McDonald KL, Portnoy DA.** *Listeria monocytogenes* triggers noncanonical autophagy upon phagocytosis, but avoids subsequent growth-restricting xenophagy. *Proc Natl Acad Sci USA.* 2018 Jan 09;115(2):E210–E217. <https://doi.org/10.1073/pnas.1716055115>
- Pereira MG, de Almeida OGG, da Silva HRA, Ishizawa MH, De Martinis ECP.** Studies on host-foodborne bacteria in intestinal three-dimensional cell culture model indicate possible mechanisms of interaction. *World J Microbiol Biotechnol.* 2021 Feb;37(2):31. <https://doi.org/10.1007/s11274-021-02996-6>
- Pizarro-Cerdá J, Cossart P.** *Listeria monocytogenes*: cell biology of invasion and intracellular growth. *Microbiol Spectr.* 2018 Nov 02;6(6):57–69. <https://doi.org/10.1128/microbiolspec.GPP3-0013-2018>
- Radoshevich L, Cossart P.** *Listeria monocytogenes*: towards a complete picture of its physiology and pathogenesis. *Nat Rev Microbiol.* 2018 Jan;16(1):32–46. <https://doi.org/10.1038/nrmicro.2017.126>
- Wang Y, Lu L, Lan R, Salazar JK, Liu J, Xu J, Ye C.** Isolation and characterization of *Listeria* species from rodents in natural environments in China. *Emerg Microbes Infect.* 2017 Jan 01;6(1):1–6. <https://doi.org/10.1038/emi.2017.28>
- Yi Z, Xie J.** Comparative proteomics reveals the spoilage-related factors of *Shewanella putrefaciens* under refrigerated condition. *Front Microbiol.* 2021 Dec 3;12:740482. <https://doi.org/10.3389/fmicb.2021.740482>
- Younis KM, Usup G, Ahmad A.** Secondary metabolites produced by marine streptomyces as antibiofilm and quorum-sensing inhibitor of uropathogen *Proteus mirabilis*. *Environ Sci Pollut Res Int.* 2016 Mar;23(5):4756–4767. <https://doi.org/10.1007/s11356-015-5687-9>